Distinct global binding patterns of the Wilms tumor gene 1 (WT1) KTS and +KTS isoforms in leukemic cells

Tove Ullmark,[1] Linnea Järvstråt,[1] Carl Sandén,[2] Giorgia Montano,[1] Helena Jernmark-Nilsson,[1] Henrik Lilljebjörn,[2] Andreas Lennartsson,[3] Thoas Fioretos,[2] Kristina Drott,[1] Karina Vidovic,[1] Björn Nilsson,[1] and Urban Gullberg[1]

[1]Division of Hematology and Transfusion Medicine, Department of Laboratory Medicine, Lund University; [2]Division of Clinical Genetics, Department of Laboratory Medicine, Lund University and [3]Department of Biosciences and Nutrition, Karolinska Institutet, Huddinge; Sweden

 doi:10.3324/haematol.2016.149815

Received: May 20, 2016.

Accepted: September 5, 2016.

Pre-published: September 9, 2016.

Correspondence: urban.gullberg@med.lu.se

Supplementary Material

Distinct global binding patterns of the Wilms' tumor gene 1 (WT1) -KTS and +KTS isoforms in leukemic cells

Tove Ullmark, Linnea Järvstråt, Carl Sandén, Giorgia Montano, Helena Jernmark-Nilsson, Henrik Lilljebjörn, Andreas Lennartsson, Thoas Fioretos, Kristina Drott, Karina Vidovic[1], Björn Nilsson, and Urban Gullberg

Supplementary Material

Ullmark et al.

1. METHODS

1.1 Cell culture

K562 cells (DSZM, German Collection of Microorganisms and Cell Cultures, Braunschweig, Germany) were cultured in RPMI 1640 medium supplemented with 10% fetal calf serum. 293T/17 cells (ATCC, LCG Standards, Wesel, Germany) were cultured in DMEM medium with 10% fetal calf serum.

1.2 Plasmids

CMV-CB6+(*WT1* +17AA/+KTS) and CMV-CB6+(*WT1* +17AA/-KTS) plasmids were provided by Dr. F. Rauscher III, Philadelphia, PA, USA; the pEF1αFlagbiotin-puro vector and the pEF1α*BirA*V5-neo vector by Dr. S. Orkin, Harvard Medical School, Boston, MA, USA; the pGL2-(*VDR*306) plasmid by Dr Holger Scholz, Berlin, Germany.

1.3 Cloning

Full length *WT1* +17AA/-KTS and *WT1* +17AA/+KTS were amplified from pCMV-CB6+(*WT1*) by PCR with these primers:
sense: 5′-CCTCAGGATATCGGTTCCGACGTTCGTGAC-3′ (*Eco*RV site underscored);
antisense: 5′-GACATTTCTAGATCAAAGCGCCAGCTGGAGTTT-3 (*Xba*1 site underscored). The PCR products were then cloned into the pEF1αFlagbiotin-puro vector and a correct reading frame was confirmed by Sanger sequencing.

1.4 Western blot

Cells were lysed with Laemmli sample buffer (Bio-Rad, Hercules, CA, USA) and sonicated using a UP50H ultrasonic homogenizer (Dr. Hielscher GmbH, Teltow, Germany). Electrophoresis using SDS-PAGE gels (Mini-Protean TGX, Bio-Rad) was followed by blotting onto Hybond ECL membranes (GE Healthcare, Amersham, UK). Pre-antibody blocking was done with 5% dry milk in TBS-T buffer. For analysis of WT1, membranes were incubated overnight with WT1 C-19 antibody (Santa Cruz Biotechnology, Dallas, TX, USA), dilution 1:500 in StartingBlock (ThermoFisher Scientific, Waltham, MA, USA), followed by a one hour incubation with goat-anti-rabbit-HRP (Bio-Rad; dilution 1:3,000 in StartingBlock). For analysis of GAPDH (Glyceraldehyde-3-Phosphate Dehydrogenase), membranes were

incubated for one hour with GAPDH 6C5 antibody (Santa Cruz Biotechnology; dilution 1:3,000 in StartingBlock), followed by one hour's incubation with goat-anti-mouse-HRP (Bio-Rad; dilution 1:3,000 in StartingBlock). For biotin detection, membranes were incubated with Streptavidin-HRP conjugate (Invitrogen, Carlsbad, CA, USA; dilution 1:20,000 in StartingBlock) for one hour. The membranes were analyzed using the EZ-ECL kit (Biological Industries, Kibbutz Beit Haemek, Israel) in a ChemiDoc MP system (Bio-Rad). The Bio-Rad Image Lab software was used for densitometry.

1.5 Luciferase assay

A luciferase reporter construct containing the minimal promoter of the *VDR* (Vitamin D Receptor), pGL2-(*VDR*306), and equal amounts of pEF1αFlagbiotin-(*WT1* +17AA/-KTS)-puro, pEF1αFlagbiotin-(*WT1* +17AA/+KTS)-puro, pcDNA3-(*WT1* +17AA/-KTS), pcDNA3-(*WT1* +17AA/+KTS), [14] or empty pcDNA3, were co-transfected into the kidney cancer cell line 293T/17, as indicated. The cultures were analyzed after 48 hours, using the Dual luciferase reporter assay (Promega, Madison, WI, USA) on a Glomax 20/20 luminometer (Turner Designs, Sunnyvale, CA, USA), according to the manufacturer's recommendations. Statistical analysis was performed using paired two-tailed t-test.

1.6 Stable transfectants

For transfection we used a previously published protocol [15] with modifications. K562 cells were electroporated at 280 V, 960 μF in a Bio-Rad GenePulser electroporator with Bio-Rad 0.4 cm cuvettes using the pEF1α*BirA*V5-neo plasmid. Transfected cells were transferred to complete medium and incubated for 24 hours before seeding 500 cells per well in 96 well plates. Subsequently, 1 mg/ml G418 was added to the cultures, and the selection pressure was then maintained throughout the cultivation of the cells. Cultures with monoclonal growth were monitored and expanded. One K562-pEF1α*BirA*V5-neo clone was chosen on the basis of stable expression of wild-type WT1 and BirA (E. coli Biotin Protein Ligase) enzyme. This clone was then electroporated as above, using pEF1αFlagbiotin-(*WT 1*+17AA/-KTS)-puro or pEF1αFlagbiotin-(*WT1* +17AA/+KTS)-puro. The seeding procedure was repeated and 24 hours after electroporation 1 μg/ml puromycin was added to the culture in addition to G418 as above. Cultures with monoclonal growth were again expanded and analyzed for protein

expression. Two clones were then chosen for subsequent ChIP-Seq analysis, aiming for expression levels of biotinylated WT1 that were comparable with those of wild-type WT1.

1.7 Validation of transgenic WT1 expression

To investigate and compare the binding patterns of WT1 isoforms with or without the KTS insertion, we made K562 clones expressing a tagged version of either of the two proteins. Both investigated isoforms retain the 17 amino acids from exon five. The first isoform used, here designated WT1 -KTS, lacks the three amino acid insert between zinc finger three and four, while the second isoform used (WT1 +KTS) retains the insert. The K562 cell line, originating from a chronic myeloid leukemia (CML) patient in blast crisis, is dependent on high levels of endogenous WT1 for survival and proliferation [Yamagami *et al.* 1996]. Western blot analysis showed that the amounts of tagged and wild-type WT1 in our clones were initially comparable (Supplementary Fig S1). The amount of endogenous WT1 protein was, however, seen to vary over time, sometimes to low levels, possibly as a result of negative feedback regulation as described [Rupprecht *et al. 1994*]. We also confirmed that the BIO-tag had been efficiently biotinylated by analyzing the blotted membranes with a streptavidin-HRP conjugate (Supplementary Fig S1). Both WT1 isoforms used were identically aminoterminally BIO-tagged. Since WT1's DNA binding zinc finger region is carboxyterminal, we did not expect interference from the aminoterminal tag with DNA binding. This assumption was confirmed by a luciferase assay using the *VDR* promoter, a known target gene of WT1 [Lee *et al.* 2001], showing similar response to tagged WT1 protein, expressed from the pEF1a plasmid, as for untagged WT1 protein (Supplementary Fig S2).

1.8 Chromatin immunoprecipitation and streptavidin capture

Chromatin immunoprecipitation was performed with nuclear extracts from the K562 clones expressing BirA and tagged WT1 +17AA/-KTS or WT1 +17AA/+KTS, and from the K562 clones expressing BirA only as background control, using the MagnaChip A/G Chromatin Immunoprecipitation Kit (Merck Millipore, Billerica, MA, USA). After crosslinking with 1% formaldehyde for 10 minutes, chromatin shearing was done by sonication in a Bioruptor UCD-200 (Diagenode, Liège, Belgium). The resulting lysate was divided into one aliquot for streptavidin capture (the equivalent of 9-10 million cells), another for Histone 3 K4 tri-

methylation (H3K4me3; ab 8580, Abcam, Cambridge, UK) immunoprecipitation (the equivalent of 1-2 million cells) and a third aliquot for non-immunoprecipitated lysate to use as input control. The H3K4me3 immunoprecipitation and the input control preparation were done using the MagnaChip kit, according to the manufacturer's instructions, increasing the reaction volumes to accommodate the input cell number. For the streptavidin capture, Dynabeads M-280 Streptavidin (Invitrogen) were used, according to the manufacturer's recommendations with minor modifications. Briefly, beads were washed with PBS three times prior to use, 3 mg of beads were used for each sample, incubation was done at room temperature, and washing after incubation was done five times with PBS with 0.1% BSA. After washing, the streptavidin beads were resuspended in Chip Elution Buffer from the MagnaChip kit and all samples proceeded to Proteinase K treatment and DNA purification according to the MagnaChip protocol.

1.9 Library preparation and sequencing

From immunoprecipitated and purified DNA, libraries were prepared using the ThruPlex DNA-seq kit (Rubicon Genomics, Ann Arbor, Michigan, USA) according to manufacturer's recommendations. Library purification was performed with a double-sided SPRI bead selection with AMPure XP beads (Agencourt, Beverly, MA) initially 0.55:1 AMPure:sample to remove the fragments above 700 bp, followed by 1:1 to bind the fragments above 200 bp, removing the free adapters. Correct fragment size distribution was ascertained using the High Sensitivity DNA Kit for the 2100 Bioanalyzer (Agilent, Santa Clara, CA, USA). The sequencing was then performed on a NextSeq 500 sequencer (Illumina, San Diego, CA, USA) using Illumina's NextSeq 500/550 High Output Kit v2 (75 cycles). Some samples were sequenced on the Illumina platform at the Science for Life Laboratory core facility in Uppsala, Sweden. Data for all samples are available in the Gene Expression Omnibus (GEO) under the accession number GSE81009.

1.10 Data analysis

Data analysis was performed as described in [Sandén *et al.* 2014]. Alignment of reads was done using the Bowtie 2 software [Langmead & Salzberg 2012]. Peak calling was performed using the MACS software [Zhang *et al.* 2008]. The peak annotation tool from the Nebula software package [Boeva *et al*. 2012] was used to find the closest gene for each peak and to determine where the peak was located in relation to that gene. Motif analysis was done with

the FIMO tool [Grant *et al.* 2011] in the MEME suite, using motifs from the TRANSFAC database [TRANSFAC 2015, Wingender *et al.* 2000]. From the same suite, DREME [Bailey 2011] was used to conduct a nonbiased motif search and TOMTOM [Gupta *et al.* 2007] was used for annotating the found motifs to known transcription factors (the TOMTOM database, however, contained no WT1 motif for comparison). Expected values for the TRANSFAC motifs were calculated by determining the number of motif occurrences within the entire genome and applying the motif density from that analysis to the length of the track, and then dividing the number of occurrences expected from the genome density by the number of peaks, to arrive at a number of expected occurrences per peak. Significance was then estimated using a simulation of 1000 tracks with peak numbers and nucleotide length to match our WT1 -KTS and WT1 +KTS peaks, calculating binomial probability of a more extreme value than the number of occurrences in our WT1 -KTS and WT1 +KTS tracks. Co-localization analysis with other K562 tracks from the ENCODE database [Gupta *et al.* 2007, ENCODE 2012, 2013] was performed as described [Sandén *et al.* 2014]. Gene ontology analysis was made using the Generic GO Term Mapper, with p-values calculated using the Generic GO Term Finder [Lewis-Siegler Inst 2016, Gene Ontology Consortium 2015]. GO results were filtered for total number of annotations in the genome, where groups with few genes (less than 100) were removed to avoid false positives. Significance of the overlap of isoform target genes was calculated using Pearson's χ^2 test with Yates correction, as was the significance of H3K4me3 enrichment around the TSS of WT1 target genes, and the significance of the enrichment for WT1 peaks seen in enhancer regions. Significance of enrichment or depletion of genomic regions for WT1 -KTS and WT1 +KTS peaks, as compared to randomized genomic positions, was also measured by Pearson's χ^2 test, with Bonferroni correction for multiple testing. 19,000 human genes [Ezkurdia *et al.* 2014] were assumed.

1.11 Comparison with Cap analysis of gene expression (CAGE) data

Cap analysis of gene expression (CAGE) data from K562 cells [FANTOM Consortium 2014] were used for a comparison between the expression levels of the WT1 target genes and those of all genes in K562 cells (defined as genes with at least one peak within the promoter area or gene body). Expression levels of each gene in the K562 cell line were calculated by adding the normalized number of transcripts from the different transcription start sites of that gene,

after which the genes were grouped into four bins: 0 (not expressed), >0-10 (low expression), >10-100 (intermediate expression), and >100 (high expression) normalized tags per million (TPM). We then compared how the target genes were distributed across the expression bins with how all genes in K562 cells were distributed across the bins. To annotate enhancer regions we compared the genomic localizations of 43,011 CAGE-derived enhancers from human cells (covering the majority of human tissues and cell types) [Andersson *et al.* 2014] to our WT1 -KTS and WT1 +KTS peaks. We considered the peak to be within the enhancer, if the peak center nucleotide was. As control we used 30,000 positions randomly distributed across the genome. Significance was calculated using the Pearson's χ^2 method with Yates correction when appropriate. The CAGE datasets used are available at http://fantom.gsc.riken.jp/5. (Accessed 27 Jan 2016).

References:

Andersson R, Gebhard C, Miguel-Escalada I, et al. FANTOM Consortium, Forrest AR, Carninci P, Rehli M, Sandelin A. An atlas of active enhancers across human cell types and tissues. Nature. 2014;507:455-61.

Bailey TL. DREME: motif discovery in transcription factor ChIP-seq data. Bioinformatics. 2011;27:1653-9.

Boeva V, Lermine A, Barette C, Guillouf C, Barillot E. Nebula--a web-server for advanced ChIP-seq data analysis. Bioinformatics. 2012;28:2517-9.

ENCODE at UCSC. ftp://hgdownload.cse.ucsc.edu/goldenPath/hg19/encodeDCC/. Accessed 14 Feb 2013.

ENCODE Project Consortium. An integrated encyclopedia of DNA elements in the human genome. Nature. 2012;489:57-74.

Ezkurdia I, Juan D, Rodriguez JM, et al. Multiple evidence strands suggest that there may be as few as 19,000 human protein-coding genes. Hum Mol Genet. 2014;23:5866-78.

FANTOM Consortium and the RIKEN PMI and CLST (DGT), Forrest AR, Kawaji H, Rehli M, et al. A promoter-level mammalian expression atlas. Nature. 2014;507:462-70.

Gene Ontology Consortium. Gene Ontology Consortium: going forward. Nucleic Acids Res. 2015;43:D1049-56.

Grant CE, Bailey TL, Noble WS. FIMO: scanning for occurrences of a given motif. Bioinformatics. 2011;27:1017-8.

Gupta S, Stamatoyannopoulos JA, Bailey TL, Noble WS. Quantifying similarity between motifs. Genome Biol. 2007;8:R24.

Langmead B, Salzberg SL. Fast gapped-read alignment with Bowtie 2. Nat Methods. 2012;9:357-9.

Lee TH, Pelletier J. Functional characterization of WT1 binding sites within the human vitamin D receptor gene promoter. Physiol Genomics. 2001;7:187-200.

Lewis-Sigler Institute for Integrative Genomics, Princeton University. http://go.princeton.edu. Accessed 14 Jan 2016.

Rupprecht HD, Drummond IA, Madden SL, Rauscher FJ 3rd, Sukhatme VP. The Wilms' tumor suppressor gene WT1 is negatively autoregulated. J Biol Chem. 1994;269:6198-206.

Sandén C, Järvstråt L, Lennartsson A, Brattås PL, Nilsson B, Gullberg U. The DEK oncoprotein binds to highly and ubiquitously expressed genes with a dual role in their transcriptional regulation. Mol Cancer. 2014;13:215.

TRANSFAC in gene-regulation.com. http://www.gene-regulation.com/pub/databases.html. Accessed 19 Jan 2015.

Wingender E, Chen X, Hehl R, et al. TRANSFAC: an integrated system for gene expression regulation. Nucleic Acids Res. 2000;28:316-9.

Yamagami T, Sugiyama H, Inoue K, et al. Growth inhibition of human leukemic cells by WT1 (Wilms tumor gene) antisense oligodeoxynucleotides: implications for the involvement of WT1 in leukemogenesis. Blood. 1996;87:2878-84.

Zhang Y, Liu T, Meyer CA, et al. Model-based analysis of ChIP-Seq (MACS). Genome Biol. 2008;9:R137.

2. TABLES

2.1 Supplementary Table S1. DNA binding motifs of WT1.

REFERENCE	MOTIF NAME	MOTIF
Rauscher et al. 1990	EGR-1 motif	CGC-CCC-CGC
Bickmore et al. 1992		GTG-AGG-CTG CTC-CCT-CCC GAG-AGG-GAG-GAT
Wang et al. 1993	(TCC)n	TCC-TCC-TCC-TCC-TCT-CC
Rupprecht et al. 1994		AGC-AGG-GGG-AGG-CT AGA-GGA-GGG-TGT-CT
Nakagama et al. 1995	WTE motif	GCG-TGG-GAG-T
Hamilton et al. 1995		GCG-TGG-GCG-(T/G)(T/A/G)(T/G)
Duarte et al. 1998		GAG-CCG-GAC
Miyamoto et al. 2008		GGA-GGA-GGG-A
Wells et al. 2010	WKE motif	ACC-AAG-CGG-GAT-GCG-GAG-CCG-CCG-CCG-CCG-CCG

The table indicates reference article, motif name where applicable, and motif. Underlining within the motif indicates stretch critical for binding.

References:

Rauscher FJ 3rd, Morris JF, Tournay OE, Cook DM, Curran T. Binding of the Wilms' tumor locus zinc finger protein to the EGR-1 consensus sequence. Science. 1990;250:1259-62.

Bickmore WA, Oghene K, Little MH, Seawright A, van Heyningen V, Hastie ND. Modulation of DNA binding specificity by alternative splicing of the Wilms tumor wt1 gene transcript. Science. 1992;257:235-7.

Wang ZY, Qiu QQ, Enger KT, Deuel TF. A second transcriptionally active DNA-binding site for the Wilms tumor gene product, WT1. Proc Natl Acad Sci U S A. 1993;90:8896-900.

Rupprecht HD, Drummond IA, Madden SL, Rauscher FJ 3rd, Sukhatme VP. The Wilms' tumor suppressor gene WT1 is negatively autoregulated. J Biol Chem. 1994;269:6198-206.

Nakagama H, Heinrich G, Pelletier J, Housman DE. Sequence and structural requirements for high-affinity DNA binding by the WT1 gene product. Mol Cell Biol. 1995;15:1489-98.

Hamilton TB, Barilla KC, Romaniuk PJ. High affinity binding sites for the Wilms' tumour suppressor protein WT1. Nucleic Acids Res. 1995;23:277-84.

Duarte A, Caricasole A, Graham CF, Ward A. Wilms' tumour-suppressor protein isoforms have opposite effects on Igf2 expression in primary embryonic cells, independently of p53 genotype. Br J Cancer. 1998;77:253-9.

Miyamoto Y, Taniguchi H, Hamel F, Silversides DW, Viger RS. A GATA4/WT1 cooperation regulates transcription of genes required for mammalian sex determination and differentiation. BMC Mol Biol. 2008;9:44.

Wells J, Rivera MN, Kim WJ, Starbuck K, Haber DA. The predominant WT1 isoform (+KTS) encodes a DNA-binding protein targeting the planar cell polarity gene Scribble in renal podocytes. Mol Cancer Res. 2010;8:975-85.

2.2. Supplementary Table S2. Complete list of significantly enriched motifs among peaks.

WT1 –KTS

	MOTIF	E-VALUE	PEAKS WITH MOTIF	TOMTOM MATCHES
1	GYGKGGGM	1.30E-267	89.9%	EGR1, EGR2
2	CCTCCYMC	9.50E-38	44.1%	SP1, ZNF263, EGR1, SP2
3	ARATA	4.30E-31	26.5%	-
4	ACTCCCAC	4.30E-31	4.2%	-
5	GGAARY	3.80E-10	58.4%	-
6	TGATWA	1.70E-09	7.7%	-
7	ABAAA	5.00E-08	47.3%	-
8	CCCCGCCC	2.50E-05	14.5%	EGR1, SP1, KLF5, SP2, KLF4, EGR2, E2F4, E2F6, E2F3, E2F1, KLF1
9	CCGCCKCC	8.40E-04	16.0%	-
10	GCYGGGA	3.40E-03	23.0%	-
11	CCCACGCR	3.60E-03	2.84%	EGR2, ARNT::AHR
12	RTGACTCA	6.20E-03	2.79%	FOSL1, JUND, JUNB, JUN::FOS, FOSL2, NFE2::MAF, JUN, BACH::MAFK, NFE2L2, FOS, BATF:JUN
13	TGACCTCW	3.20E-02	2.95%	Rxra, RXR::RAR, NR2C2, PPARG::RXRA, NR1H2:RXRA, NR1H3:RXRA, NR2F1

WT1 +KTS

	MOTIF	E-VALUE	PEAKS WITH MOTIF	TOMTOM MATCHES
1	TAWTTTTW	1.4e-2917	35.5%	-
2	TARTCCCA	1.5e-2706	40.0%	-
3	GAGGCBGA	1.0e-2550	50.3%	-
4	CAGGAGAW	2.4e-2412	42.5%	-
5	GGKTTCAY	9.3e-2463	42.0%	-
6	GTKAGCCR	1.6e-2118	42.2%	-
7	GTAGAGAY	1.7e-2064	31.9%	-
8	CGCCCGSC	1.0e-1864	35.3%	-
9	GCTACTY	4.2e-1661	38.9%	-
10	TGCAGTGR	3.1e-1496	36.2%	-
11	AGGCTGGA	2.8e-1133	27.2%	-
12	CGYGATC	1.6e-1053	23.6%	-
13	CGAGACY	3.9e-1025	29.4%	-
14	GGGYGACA	2.7e-805	20.0%	-
15	GCTTGCA	1.6e-709	29.6%	-
16	CACTTTGG	3.8e-506	12.0%	-
17	ACCAYGCC	2.6e-487	14.6%	-
18	RTCTCAAA	2.6e-450	10.3%	-
19	CRGGYGCC	4.3e-405	25.9%	-
20	AAAAHAMA	6.7e-293	15.6%	-
21	GCKTGAAC	1.5e-289	8.1%	-
22	AGATDGCG	2.1e-224	8.0%	-
23	CGTKTTAG	8.7e-217	5.6%	-
24	AGACCATC	2.9e-160	4.6%	-
25	AGATCCCG	6.4e-121	3.9%	-
26	GAGGCAGA	4.0e-112	8.4%	-

Complete list of significantly enriched motifs found among peaks. Partial lists are found in Table 2 and Table 3, respectively.

Supplementary Material

Ullmark et al.

2.3 Supplementary Table S3. Enriched "Process" GO groups for WT1 -KTS and +KTS.

			WT1 –KTS			WT1 +KTS		
GOID	**TERM**	**Genome frequency**	**Cluster frequency**	**Fold change**	**p-value**	**Cluster frequency**	**Fold change**	**p-value**
GO:0048856	anatomical structure development	12.46%	34.15%	2.58	7.50E-75	31.13%	2.50	3.65E-313
GO:0006950	response to stress	10.78%	24.12%	2.09	1.88E-33	22.59%	2.10	9.17E-144
GO:0030154	cell differentiation	8.90%	27.55%	2.93	1.11E-69	22.99%	2.58	7.82E-235
GO:0002376	immune system process	7.03%	16.62%	2.44	1.60E-26	-	-	-
GO:0022607	cellular component assembly	6.64%	14.45%	2.09	1.73E-17	16.18%	2.44	3.28E-139
GO:0009056	catabolic process	5.94%	-	-	-	12.97%	2.18	3.07E-85
GO:0008219	cell death	5.00%	14.27%	2.74	7.25E-29	11.86%	2.37	3.87E-94
GO:0007049	cell cycle	4.84%	13.01%	2.46	8.06E-21	12.17%	2.51	1.70E-109
GO:0016192	vesicle-mediated transport	4.62%	-	-	-	9.46%	2.05	3.14E-50
GO:0008283	cell proliferation	4.57%	12.92%	2.88	4.32E-26	10.77%	2.36	2.32E-83
GO:0065003	macromolecular complex assembly	4.49%	9.76%	2.22	4.60E-11	10.33%	2.30	1.76E-74
GO:0040011	locomotion	4.40%	13.82%	3.04	2.76E-32	11.77%	2.68	1.98E-119
GO:0007155	cell adhesion	4.25%	8.76%	2.14	6.28E-09	9.99%	2.35	2.48E-76
GO:0042592	homeostatic process	3.89%	9.94%	2.60	6.13E-16	8.84%	2.27	5.23E-62
GO:0007010	cytoskeleton organization	3.87%	10.03%	2.46	5.40E-16	7.83%	2.02	5.44E-40
GO:0006461	protein complex assembly	3.82%	8.67%	2.37	2.34E-10	8.70%	2.28	9.64E-61
GO:0000902	cell morphogenesis	3.52%	11.20%	2.95	4.96E-25	10.64%	3.02	2.38E-134
GO:0051276	chromosome organization	3.30%	-	-	-	7.32%	2.22	5.47E-47
GO:0048870	cell motility	3.19%	9.49%	2.91	2.47E-20	8.32%	2.61	3.67E-78
GO:0000003	reproduction	3.17%	6.50%	2.09	5.83E-05	7.41%	2.34	1.54E-54
GO:0007267	cell-cell signaling	2.93%	8.76%	2.57	1.51E-16	6.63%	2.26	6.14E-45
GO:0048646	anatomical structure formation involved in morphogenesis	2.84%	8.22%	2.87	2.36E-15	7.54%	2.65	5.98E-73
GO:0061024	membrane organization	2.81%	7.23%	3.14	4.69E-08	7.19%	2.56	2.25E-64
GO:0040007	growth	2.33%	6.32%	2.91	8.46E-11	6.07%	2.61	6.13E-56
GO:0009790	embryo development	2.29%	7.86%	3.40	7.31E-19	6.03%	2.63	1.70E-56
GO:0044403	symbiosis, encompassing mutualism through parasitism	2.00%	4.88%	2.52	2.65E-05	4.40%	2.20	1.07E-26
GO:0007005	mitochondrion organization	1.73%	4.16%	2.09	3.35E-03	3.69%	2.13	6.58E-20
GO:0051301	cell division	1.69%	5.06%	3.18	1.28E-09	4.76%	2.82	2.93E-50
GO:0006605	protein targeting	1.63%	4.34%	2.39	5.89E-05	3.67%	2.25	1.36E-22
GO:0003013	circulatory system process	1.17%	-	-	-	3.25%	2.78	1.31E-32
GO:0006914	autophagy	1.16%	-	-	-	3.12%	2.69	1.30E-28
GO:0007067	mitotic nuclear division	1.12%	2.98%	2.69	4.22E-04	3.27%	2.92	3.71E-36
GO:0006913	nucleocytoplasmic transport	1.02%	3.79%	3.47	1.95E-08	2.43%	2.38	6.91E-17
GO:0006790	sulfur compound metabolic process	1.01%	-	-	-	2.34%	2.32	5.45E-15
GO:0034655	nucleobase-containing compound catabolic process	0.99%	-	-	-	2.02%	2.04	1.74E-08
GO:0051604	protein maturation	0.87%	-	-	-	2.00%	2.30	2.90E-12
GO:0030198	extracellular matrix organization	0.86%	2.44%	3.24	3.63E-05	2.40%	2.79	2.28E-23
GO:0007059	chromosome segregation	0.76%	-	-	-	1.91%	2.51	1.82E-14
GO:0007009	plasma membrane organization	0.69%	2.53%	3.14	3.73E-04	2.02%	2.93	3.57E-21
GO:0007568	aging	0.66%	2.35%	4.18	1.57E-05	1.47%	2.23	1.85E-07
GO:0034330	cell junction organization	0.61%	2.08%	3.42	2.05E-03	2.11%	3.46	9.96E-30
GO:0021700	developmental maturation	0.57%	1.90%	3.55	5.86E-03	1.47%	2.58	2.72E-11
GO:0022618	ribonucleoprotein complex assembly	0.56%	-	-	-	1.29%	2.30	1.29E-06
GO:0030705	cytoskeleton-dependent intracellular transport	0.30%	-	-	-	1.05%	3.50	7.90E-14
GO:0043473	pigmentation	0.22%	-	-	-	0.64%	2.91	9.47E-05

The genes with peaks inside the gene body or in the promoter area were subjected to Gene Ontology analysis using the Generic GO Term Mapper (http://go.princeton.edu. Accessed 14 Jan 2016; Gene Ontology Consortium. Gene Ontology Consortium: going forward. Nucleic Acids Res. 2015;43:D1049-56) , with the "Process" setting. The list is manually curated, removing GO terms with fewer than 100 genes annotated in the whole genome to avoid false positives. Cut-off was set at fold enrichment >2. Calculation of p-values using the Generic GO Term Finder tool.

Supplementary Material

Ullmark et al.

2.4 Supplementary Table S4. Enriched "Function" GO groups for WT1 -KTS and +KTS.

			WT1 -KTS			WT1 +KTS		
GOID	**TERM**	**Genome frequency**	**Cluster frequency**	**Fold change**	**p-value**	**Cluster frequency**	**Fold change**	**p-value**
GO:0032182	ubiquitin-like protein binding	0.25%	-	-	-	0.87%	3.48	5.21E-12
GO:0042393	histone binding	0.39%	1.26%	3.70	0.0137	1.31%	3.36	6.46E-17
GO:0030674	protein binding, bridging	0.37%	1.72%	4.76	0.0001	1.20%	3.24	1.02E-14
GO:0019899	enzyme binding	4.09%	13.19%	2.97	3.53E-31	12.33%	3.01	6.75E-157
GO:0000988	transcription factor activity, protein binding	1.57%	4.43%	2.72	5.43E-08	3.72%	2.37	2.91E-27
GO:0008134	transcription factor binding	1.29%	5.15%	3.56	4.57E-15	3.03%	2.35	1.41E-21
GO:0030234	enzyme regulator activity	3.08%	-	-	-	6.27%	2.04	1.56E-32
GO:0016874	ligase activity	1.52%	-	-	-	3.05%	2.01	4.87E-14
GO:0008092	cytoskeletal protein binding	3.27%	6.96%	2.23	1.15E-07	-	-	-
GO:0003723	RNA binding	4.82%	10.30%	2.16	7.50E-11	-	-	-
GO:0003677	DNA binding	8.39%	17.62%	2.10	2.90E-19	-	-	-
GO:0032182	ubiquitin-like protein binding	0.25%	-	-	-	0.87%	3.48	5.21E-12

The target genes with peaks within the gene body or promoter area were subjected to Gene Ontology analysis in the Generic GO Term Mapper (http://go.princeton.edu. Accessed 14 Jan 2016; Gene Ontology Consortium. Gene Ontology Consortium: going forward. Nucleic Acids Res. 2015;43:D1049-56), using the "Function" setting. The list is manually curated, removing terms with fewer than 100 genes annotated in the genome to avoid false positives. Cut-off was set at fold enrichment >2. Calculation of p-values through Generic GO Term Finder analysis.

2.5 Supplementary Table S5. Complete list of ENCODE ChIP-Seq tracks with significant similarity to -KTS (S5A) and +KTS (S%B) WT1 peaks.

Table S5A, WT1 -KTS

	Track	Similarity score	p-value
1	wgEncodeHaibTfbsK562Egr1V0416101PkRep1	0.108274	9.99E-04
2	wgEncodeHaibTfbsK562Cbx3sc101004V0422111PkRep1	0.058714	9.99E-04
3	wgEncodeHaibTfbsK562Zbtb7asc34508V0416101PkRep2	0.056838	9.99E-04
4	wgEncodeOpenChromDnaseK562G1phasePk	0.04972	9.99E-04
5	wgEncodeOpenChromDnaseK562G2mphasePk	0.049081	9.99E-04
6	wgEncodeOpenChromDnaseK562PkV2	0.048757	9.99E-04
7	wgEncodeHaibTfbsK562Hey1Pcr1xPkRep1	0.048251	9.99E-04
8	wgEncodeHaibTfbsK562MaxV0416102PkRep2	0.047713	9.99E-04
9	wgEncodeOpenChromDnaseK562SahactrlPk	0.047693	9.99E-04
10	wgEncodeOpenChromDnaseK562Saha1u72hrPk	0.047583	9.99E-04
11	wgEncodeOpenChromDnaseK562NabutPk	0.045986	9.99E-04
12	wgEncodeOpenChromDnaseK562Pk	0.044686	9.99E-04
13	wgEncodeHaibTfbsK562MaxV0416102PkRep1	0.042228	9.99E-04
14	wgEncodeHaibTfbsK562E2f6sc22823V0416102PkRep2	0.041029	9.99E-04
15	wgEncodeHaibTfbsK562E2f6V0416102PkRep2	0.041029	9.99E-04
16	wgEncodeOpenChromChipK562CmycPk	0.040484	9.99E-04
17	wgEncodeHaibTfbsK562Hey1Pcr1xPkRep2	0.037512	9.99E-04
18	wgEncodeOpenChromSynthK562Pk	0.035282	9.99E-04
19	wgEncodeOpenChromFaireK562Pk	0.034536	9.99E-04
20	wgEncodeUwDnaseK562Znfp5PkRep1	0.032372	9.99E-04
21	wgEncodeBroadHistoneK562H2azStdPk	0.028038	9.99E-04
22	wgEncodeHaibTfbsK562Elf1sc631V0416102PkRep2	0.027557	9.99E-04
23	wgEncodeHaibTfbsK562CtcfcPcr1xPkRep1V2	0.027416	9.99E-04
24	wgEncodeBroadHistoneK562H3k9acStdPk	0.026666	9.99E-04
25	wgEncodeBroadHistoneK562H3k27acStdPk	0.024309	9.99E-04
26	wgEncodeOpenChromChipK562Pol2Pk	0.024301	9.99E-04
27	wgEncodeUwDnaseK562Znfp5PkRep2	0.023463	9.99E-04
28	wgEncodeBroadHistoneK562Phf8a301772aStdPk	0.02297	9.99E-04
29	wgEncodeHaibTfbsK562Egr1V0416101PkRep2	0.02153	9.99E-04
30	wgEncodeHaibTfbsK562CtcfcPcr1xPkRep1	0.020653	9.99E-04
31	wgEncodeBroadHistoneK562H3k4me2StdPk	0.020088	9.99E-04
32	wgEncodeBroadHistoneK562H3k4me3StdPk	0.019521	9.99E-04
33	wgEncodeHaibTfbsK562Pu1Pcr1xPkRep1	0.019174	9.99E-04
34	wgEncodeUwDnaseK562Znf4c50c4PkRep2	0.019077	9.99E-04
35	wgEncodeUchicagoTfbsK562EjundControlPk	0.018769	9.99E-04
36	wgEncodeBroadHistoneK562Rbbp5a300109aStdPk	0.018134	9.99E-04
37	wgEncodeAwgDnaseUwdukeK562UniPk	0.01801	9.99E-04
38	wgEncodeHaibTfbsK562Rad21V0416102PkRep2	0.017132	9.99E-04
39	wgEncodeHaibTfbsK562Nr2f2sc271940V0422111PkRep2	0.016611	9.99E-04
40	wgEncodeBroadHistoneK562Hdac1sc6298StdPk	0.016323	9.99E-04
41	wgEncodeHaibTfbsK562Hdac2sc6296V0416102PkRep1	0.016122	9.99E-04
42	wgEncodeHaibTfbsK562Nr2f2sc271940V0422111PkRep1	0.015803	9.99E-04
43	wgEncodeUwDnaseK562Znf4c50c4PkRep1	0.014673	9.99E-04
44	wgEncodeUwDnaseK562Znfe103c6PkRep2	0.014565	9.99E-04

45	wgEncodeBroadHistoneK562Plu1StdPk	0.014374	9.99E-04
46	wgEncodeBroadHistoneK562Pol2bStdPk	0.014148	9.99E-04
47	wgEncodeBroadHistoneK562Sap3039731StdPk	0.01414	9.99E-04
48	wgEncodeUwDnaseK562PkRep1	0.014112	9.99E-04
49	wgEncodeHaibTfbsK562Atf3V0416101PkRep1	0.013532	9.99E-04
50	wgEncodeUwDnaseK562Znfg54a11PkRep1	0.012987	9.99E-04
51	wgEncodeBroadHistoneK562Hdac2a300705aStdPk	0.012792	9.99E-04
52	wgEncodeUwDnaseK562Znfb34a8PkRep2	0.012207	9.99E-04
53	wgEncodeBroadHistoneK562Setdb1Pk	0.012126	9.99E-04
54	wgEncodeBroadHistoneK562H3k4me1StdPk	0.011663	9.99E-04
55	wgEncodeHaibTfbsK562CtcfcPcr1xPkRep2	0.011624	9.99E-04
56	wgEncodeSydhTfbsK562Ccnt2StdPk	0.010901	9.99E-04
57	wgEncodeUwDnaseK562Znf4g7d3PkRep2	0.010817	9.99E-04
58	wgEncodeBroadHistoneK562Chd7a301223a1Pk	0.010807	9.99E-04
59	wgEncodeUwDnaseK562Znfg54a11PkRep2	0.010792	9.99E-04
60	wgEncodeHaibTfbsK562Cbx3sc101004V0422111PkRep2	0.010496	9.99E-04
61	wgEncodeUwDnaseK562Znfa41c6PkRep1	0.010359	9.99E-04
62	wgEncodeSydhTfbsK562Hmgn3StdPk	0.010308	9.99E-04
63	wgEncodeUwHistoneK562H3k04me3StdZnff41b2PkRep1	0.010229	9.99E-04
64	wgEncodeBroadHistoneK562CtcfStdPk	0.009985	9.99E-04
65	wgEncodeHaibTfbsK562Rad21V0416102PkRep1	0.00998	9.99E-04
66	wgEncodeHaibTfbsK562Ets1V0416101PkRep2	0.009918	9.99E-04
67	wgEncodeUwDnaseK562Znff41b2PkRep2	0.009841	9.99E-04
68	wgEncodeOpenChromChipK562CtcfPk	0.009818	9.99E-04
69	wgEncodeHaibTfbsK562Stat5asc74442V0422111PkRep1	0.009385	9.99E-04
70	wgEncodeUwTfbsK562CtcfStdPkRep1	0.009328	9.99E-04
71	wgEncodeHaibTfbsK562GabpV0416101PkRep1	0.009267	9.99E-04
72	wgEncodeHaibTfbsK562Trim28sc81411V0422111PkRep1	0.00925	9.99E-04
73	wgEncodeUwHistoneK562H3k04me3StdZnfp5PkRep1	0.00903	9.99E-04
74	wgEncodeHaibTfbsK562Yy1V0416102PkRep2	0.008587	9.99E-04
75	wgEncodeUwHistoneK562H3k04me3StdZnf4c50c4PkRep1	0.008566	9.99E-04
76	wgEncodeBroadHistoneK562Hdac6a301341aPk	0.008464	9.99E-04
77	wgEncodeBroadHistoneK562H3k9me1StdPk	0.008357	9.99E-04
78	wgEncodeBroadHistoneK562Sirt6Pk	0.008239	9.99E-04
79	wgEncodeBroadHistoneK562P300StdPk	0.008212	9.99E-04
80	wgEncodeHaibTfbsK562Tead4sc101184V0422111PkRep2	0.008182	9.99E-04
81	wgEncodeSydhTfbsK562Mazab85725IggrabPk	0.008166	9.99E-04
82	wgEncodeUwHistoneK562H3k04me3StdZnff41b2PkRep2	0.008135	9.99E-04
83	wgEncodeBroadHistoneK562Ezh239875StdPk	0.008133	9.99E-04
84	wgEncodeUwDnaseK562Znfe103c6PkRep1	0.008127	9.99E-04
85	wgEncodeSydhTfbsK562Znfmizdcp1ab65767IggrabPk	0.008123	9.99E-04
86	wgEncodeUwHistoneK562H3k4me3StdPkRep2	0.007961	9.99E-04
87	wgEncodeBroadHistoneK562H3k79me2StdPk	0.007897	9.99E-04
88	wgEncodeBroadHistoneK562Chd1a301218aStdPk	0.007777	9.99E-04
89	wgEncodeUwTfbsK562CtcfStdPkRep2	0.00777	9.99E-04
90	wgEncodeHaibTfbsK562Elf1sc631V0416102PkRep1	0.007718	9.99E-04
91	wgEncodeHaibTfbsK562Zbtb7asc34508V0416101PkRep1	0.007623	9.99E-04
92	wgEncodeUwHistoneK562H3k4me3StdPkRep1	0.007619	9.99E-04
93	wgEncodeUwDnaseK562Znf4g7d3PkRep1	0.007561	9.99E-04
94	wgEncodeHaibTfbsK562Cebpdsc636V0422111PkRep1	0.007556	9.99E-04
95	wgEncodeUwHistoneK562H3k04me3StdZnfp5PkRep2	0.007495	9.99E-04
96	wgEncodeSydhTfbsK562Bhlhe40nb100IggrabPk	0.007353	9.99E-04
97	wgEncodeUwHistoneK562H3k04me3StdZnf2c10c5PkRep1	0.00734	9.99E-04
97	wgEncodeHaibTfbsK562Yy1sc281V0416101PkRep1	0.007334	9.99E-04
99	wgEncodeHaibTfbsK562Yy1V0416101PkRep1	0.007334	9.99E-04
100	wgEncodeHaibTfbsK562Tead4sc101184V0422111PkRep1	0.007254	9.99E-04

101	wgEncodeHaibTfbsK562Pol2V0416101PkRep2	0.007192	9.99E-04
102	wgEncodeSydhTfbsK562Cmyclfng30StdPk	0.007142	9.99E-04
103	wgEncodeHaibTfbsK562Pol24h8V0416101PkRep2	0.007074	9.99E-04
104	wgEncodeSydhTfbsK562Corestab24166IggrabPk	0.00703	9.99E-04
105	wgEncodeBroadHistoneK562Suz12051317Pk	0.006948	9.99E-04
106	wgEncodeHaibTfbsK562Taf1V0416101PkRep1	0.006913	9.99E-04
107	wgEncodeBroadHistoneK562Lsd1Pk	0.006844	9.99E-04
108	wgEncodeBroadHistoneK562Nsd2ab75359Pk	0.006835	9.99E-04
109	wgEncodeUwHistoneK562H3k04me3StdZnfa41c6PkRep2	0.006805	9.99E-04
110	wgEncodeHaibTfbsK562Pol2V0416101PkRep1	0.006658	9.99E-04
111	wgEncodeUwHistoneK562H3k04me3StdZnf4c50c4PkRep2	0.006639	9.99E-04
112	wgEncodeSydhTfbsK562Tblr1ab24550IggrabPk	0.00662	9.99E-04
113	wgEncodeUwHistoneK562H3k04me3StdZnf2c10c5PkRep2	0.006513	9.99E-04
114	wgEncodeSydhTfbsK562MaxIggrabPk	0.006423	9.99E-04
115	wgEncodeHaibTfbsK562Cebpbsc150V0422111PkRep2	0.006379	9.99E-04
116	wgEncodeSydhTfbsK562P300IggrabPk	0.006374	9.99E-04
117	wgEncodeSydhTfbsK562Corestsc30189IggrabPk	0.006323	9.99E-04
118	wgEncodeSydhTfbsK562CmycIggrabPk	0.006249	9.99E-04
119	wgEncodeUwDnaseK562Znfa41c6PkRep2	0.006105	9.99E-04
120	wgEncodeBroadHistoneK562Cbx3sc101004Pk	0.006104	9.99E-04
121	wgEncodeHaibTfbsK562Hdac2sc6296V0416102PkRep2	0.006056	9.99E-04
122	wgEncodeHaibTfbsK562Pmlsc71910V0422111PkRep2	0.005808	9.99E-04
123	wgEncodeSydhTfbsK562Pol2StdPk	0.005806	9.99E-04
124	wgEncodeSydhTfbsK562Irf1Ifng6hStdPk	0.005663	9.99E-04
125	wgEncodeHaibTfbsK562Sin3ak20V0416101PkRep2	0.005656	9.99E-04
126	wgEncodeHaibTfbsK562GabpV0416101PkRep2	0.005639	9.99E-04
127	wgEncodeUwDnaseK562Znfb34a8PkRep1	0.005593	9.99E-04
128	wgEncodeHaibTfbsK562Taf1V0416101PkRep2	0.005586	9.99E-04
129	wgEncodeSydhTfbsK562JundIggrabPk	0.005568	9.99E-04
130	wgEncodeUwDnaseK562Znff41b2PkRep1	0.005528	9.99E-04
131	wgEncodeSydhTfbsK562E2f6UcdPk	0.005393	9.99E-04
132	wgEncodeSydhTfbsK562Ubtfsab1404509IggmusPk	0.005375	9.99E-04
133	wgEncodeHaibTfbsK562Cebpbsc150V0422111PkRep1	0.005321	9.99E-04
134	wgEncodeSydhTfbsK562Stat2Ifna30StdPk	0.005293	9.99E-04
135	wgEncodeHaibTfbsK562Pol24h8V0416101PkRep1	0.005273	9.99E-04
136	wgEncodeHaibTfbsK562E2f6sc22823V0416102PkRep1	0.005192	9.99E-04
137	wgEncodeHaibTfbsK562E2f6V0416102PkRep1	0.005192	9.99E-04
138	wgEncodeHaibTfbsK562NrsfV0416102PkRep1	0.005136	9.99E-04
139	wgEncodeBroadHistoneK562Cbx8Pk	0.005083	9.99E-04
140	wgEncodeUchicagoTfbsK562EjunbControlPk	0.005079	9.99E-04
141	wgEncodeHaibTfbsK562Gata2sc267Pcr1xPkRep1	0.005062	9.99E-04
142	wgEncodeSydhTfbsK562Pol2Ifng6hStdPk	0.005045	9.99E-04
143	wgEncodeSydhTfbsK562Tblr1nb600270IggrabPk	0.004997	9.99E-04
144	wgEncodeSydhTfbsK562Gtf2f1ab28179IggrabPk	0.00497	9.99E-04
145	wgEncodeBroadHistoneK562Chd4mi2Pk	0.004964	9.99E-04
146	wgEncodeHaibTfbsK562Ets1V0416101PkRep1	0.004833	9.99E-04
147	wgEncodeSydhTfbsK562Pol2IggmusPk	0.004826	9.99E-04
148	wgEncodeSydhTfbsK562Pol2Ifng30StdPk	0.004795	9.99E-04
149	wgEncodeBroadHistoneK562H4k20me1StdPk	0.004779	9.99E-04
150	wgEncodeHaibTfbsK562Usf1V0416101PkRep1	0.004725	9.99E-04
151	wgEncodeSydhTfbsK562Mxi1af4185IggrabPk	0.004694	9.99E-04
152	wgEncodeSydhTfbsK562Chd2ab68301IggrabPk	0.004645	2.00E-03
153	wgEncodeHaibTfbsK562Ctcflsc98982V0416101PkRep1	0.004582	9.99E-04
154	wgEncodeSydhTfbsK562Hcfc1nb10068209IggrabPk	0.00455	9.99E-04
155	wgEncodeSydhTfbsK562Znf143IggrabPk	0.004536	9.99E-04
156	wgEncodeUchicagoTfbsK562Ehdac8ControlPk	0.004484	9.99E-04

157	wgEncodeSydhTfbsK562CmycIfng6hStdPk	0.004375	9.99E-04
158	wgEncodeSydhTfbsK562Gtf2bStdPk	0.004363	9.99E-04
159	wgEncodeUchicagoTfbsK562Enr4a1ControlPk	0.004281	9.99E-04
160	wgEncodeSydhTfbsK562Zc3h11anb10074650IggrabPk	0.004277	9.99E-04
161	wgEncodeSydhTfbsK562Stat1Ifng6hStdPk	0.004246	9.99E-04
162	wgEncodeSydhTfbsK562E2f4UcdPk	0.004207	9.99E-04
163	wgEncodeSydhTfbsK562Ubfsc13125IggmusPk	0.004141	9.99E-04
164	wgEncodeBroadHistoneK562H3k9me3StdPk	0.004099	9.99E-04
165	wgEncodeSydhTfbsK562Stat1Ifna30StdPk	0.004074	9.99E-04
166	wgEncodeSydhTfbsK562CjunIggrabPk	0.004012	9.99E-04
167	wgEncodeUchicagoTfbsK562Egata2ControlPk	0.003992	9.99E-04
168	wgEncodeUwDnaseK562PkRep2	0.003846	9.99E-04
169	wgEncodeSydhTfbsK562Gata2UcdPk	0.003826	9.99E-04
170	wgEncodeUwHistoneK562H3k04me3StdZnfa41c6PkRep1	0.00379	9.99E-04
171	wgEncodeSydhTfbsK562P300sc584sc48343IggrabPk	0.003783	9.99E-04
172	wgEncodeHaibTfbsK562Pmlsc71910V0422111PkRep1	0.003761	9.99E-04
173	wgEncodeSydhHistoneK562bH3k9acbUcdPk	0.003711	9.99E-04
174	wgEncodeSydhHistoneK562H3k9acbUcdPk	0.003711	9.99E-04
175	wgEncodeUchicagoTfbsK562EfosControlPk	0.003659	9.99E-04
176	wgEncodeSydhTfbsK562Tal1sc12984IggmusPk	0.003583	9.99E-04
177	wgEncodeSydhTfbsK562TbpIggmusPk	0.003571	9.99E-04
178	wgEncodeUwDnaseK562Znf2c10c5PkRep1	0.003541	9.99E-04
179	wgEncodeSydhTfbsK562Pol2Ifna30StdPk	0.003518	9.99E-04
180	wgEncodeHaibTfbsK562Pu1Pcr1xPkRep2	0.003335	9.99E-04
181	wgEncodeHaibTfbsK562Yy1V0416102PkRep1	0.003269	9.99E-04
182	wgEncodeSydhTfbsK562Arid3asc8821IggrabPk	0.003249	9.99E-04
183	wgEncodeSydhHistoneK562bH3k4me1UcdPk	0.003186	9.99E-04
184	wgEncodeSydhHistoneK562H3k4me1UcdPk	0.003186	9.99E-04
185	wgEncodeSydhTfbsK562CmycStdPk	0.003111	9.99E-04
186	wgEncodeHaibTfbsK562NrsfV0416102PkRep2	0.003062	9.99E-04
187	wgEncodeSydhHistoneK562bH3k4me3bUcdPk	0.002948	9.99E-04
188	wgEncodeSydhHistoneK562H3k4me3bUcdPk	0.002948	9.99E-04
189	wgEncodeBroadHistoneK562Rnf2Pk	0.002889	9.99E-04
190	wgEncodeOpenChromFaireK562NabutPk	0.002806	9.99E-04
191	wgEncodeSydhTfbsK562Elk112771IggrabPk	0.002603	2.00E-03
192	wgEncodeSydhTfbsK562Smc3ab9263IggrabPk	0.00259	2.00E-03
193	wgEncodeSydhTfbsK562CtcfbIggrabPk	0.002555	2.00E-03
194	wgEncodeHaibTfbsK562Fosl1sc183V0416101PkRep1	0.002542	2.00E-03
195	wgEncodeHaibTfbsK562Stat5asc74442V0422111PkRep2	0.002516	9.99E-04
196	wgEncodeSydhTfbsK562Znf384hpa004051IggrabPk	0.002406	9.99E-04
197	wgEncodeHaibTfbsK562Ctcflsc98982V0416101PkRep2	0.002392	9.99E-04
197	wgEncodeHaibTfbsK562Sp1Pcr1xPkRep2	0.002352	9.99E-04
199	wgEncodeBroadHistoneK562NcorPk	0.00234	9.99E-04
201	wgEncodeHaibTfbsK562Atf3V0416101PkRep2	0.002254	9.99E-04
202	wgEncodeBroadHistoneK562PcafPk	0.002221	9.99E-04
203	wgEncodeUwDnaseK562Znf2c10c5PkRep2	0.002218	9.99E-04
204	wgEncodeHaibTfbsK562Creb1sc240V0422111PkRep1	0.002204	9.99E-04
205	wgEncodeSydhTfbsK562Cdpsc6327IggrabPk	0.002169	9.99E-04
206	wgEncodeSydhTfbsK562Pol2Ifna6hStdPk	0.002145	9.99E-04
207	wgEncodeBroadHistoneK562H3k27me3StdPk	0.002125	9.99E-04
208	wgEncodeHaibTfbsK562Six5V0416101PkRep2	0.002067	9.99E-04
209	wgEncodeHaibTfbsK562Yy1sc281V0416101PkRep2	0.002039	9.99E-04
210	wgEncodeHaibTfbsK562Yy1V0416101PkRep2	0.002039	9.99E-04
211	wgEncodeHaibTfbsK562Gata2sc267Pcr1xPkRep2	0.002025	9.99E-04
212	wgEncodeSydhTfbsK562CmycIfna6hStdPk	0.002003	9.99E-04
213	wgEncodeBroadHistoneK562H3k36me3StdPk	0.001912	9.99E-04

214	wgEncodeHaibTfbsK562Trim28sc81411V0422111PkRep2	0.001831	9.99E-04
215	wgEncodeHaibMethyl450K562SitesRep1	0.001827	9.99E-04
216	wgEncodeHaibTfbsK562Sp2sc643V0416102PkRep2	0.001811	9.99E-04
217	wgEncodeSydhTfbsK562Bach1sc14700IggrabPk	0.001793	9.99E-04
218	wgEncodeHaibTfbsK562SrfV0416101PkRep1	0.001759	9.99E-04
219	wgEncodeSydhTfbsK562Mafkab50322IggrabPk	0.00169	3.00E-03
220	wgEncodeSydhTfbsK562Nrf1IggrabPk	0.001671	9.99E-04
221	wgEncodeHaibTfbsK562Thap1sc98174V0416101PkRep1	0.001651	9.99E-04
222	wgEncodeHaibTfbsK562Fosl1sc183V0416101PkRep2	0.00163	2.00E-03
223	wgEncodeHaibTfbsK562Sp2sc643V0416102PkRep1	0.001586	9.99E-04
224	wgEncodeBroadHistoneK562Cbpsc369Pk	0.001563	3.00E-03
225	wgEncodeHaibTfbsK562Zbtb33Pcr1xPkRep2	0.001552	9.99E-04
226	wgEncodeSydhTfbsK562Stat1Ifna6hStdPk	0.001453	2.00E-03
227	wgEncodeSydhTfbsK562CebpbIggrabPk	0.001438	9.99E-04
228	wgEncodeHaibTfbsK562Usf1V0416101PkRep2	0.001417	9.99E-04
229	wgEncodeSydhTfbsK562NfyaStdPk	0.00138	9.99E-04
230	wgEncodeSydhTfbsK562Brf1StdPk	0.001333	5.00E-03
231	wgEncodeHaibTfbsK562Cebpdsc636V0422111PkRep2	0.001273	9.99E-04
232	wgEncodeHaibTfbsK562Six5Pcr1xPkRep1	0.001246	2.00E-03
233	wgEncodeSydhTfbsK562Irf1Ifng30StdPk	0.001236	9.99E-04
234	wgEncodeSydhTfbsK562CjunStdPk	0.001205	9.99E-04
235	wgEncodeSydhTfbsK562Rfx5IggrabPk	0.001164	9.99E-04
236	wgEncodeSydhTfbsK562Gata1bIggmusPk	0.001126	9.99E-04
237	wgEncodeHaibTfbsK562Creb1sc240V0422111PkRep2	0.001109	2.00E-03
238	wgEncodeSydhTfbsK562CjunIfna30StdPk	0.001104	3.00E-03
239	wgEncodeSydhTfbsK562Yy1UcdPk	0.001094	9.99E-04
240	wgEncodeHaibTfbsK562Zbtb33Pcr1xPkRep1	0.00106	9.99E-04
241	wgEncodeSydhTfbsK562CfosStdPk	0.001011	2.00E-03
242	wgEncodeSydhTfbsK562Usf2IggrabPk	0.000998	9.99E-04
243	wgEncodeSydhTfbsK562Atf106325StdPk	0.000984	9.99E-04
244	wgEncodeSydhTfbsK562Irf1Ifna6hStdPk	0.000968	9.99E-04
245	wgEncodeHaibTfbsK562Sp1Pcr1xPkRep1	0.000962	3.00E-03
246	wgEncodeHaibTfbsK562Thap1sc98174V0416101PkRep2	0.000949	5.00E-03
247	wgEncodeSydhTfbsK562Tr4UcdPk	0.000864	9.99E-04
248	wgEncodeSydhTfbsK562CmycIfna30StdPk	0.000852	9.99E-04
249	wgEncodeSydhTfbsK562MaxStdPk	0.000833	9.99E-04
250	wgEncodeHaibMethylRrbsK562HaibSitesRep1	0.000832	9.99E-04
251	wgEncodeHaibMethylRrbsK562HudsonalphagrowprotSitesRep1	0.000832	9.99E-04
252	wgEncodeSydhTfbsK562Stat1Ifng30StdPk	0.000811	2.00E-03
253	wgEncodeSydhTfbsK562NfybStdPk	0.000806	5.00E-03
254	wgEncodeHaibTfbsK562Six5V0416101PkRep1	0.000805	2.00E-03
255	wgEncodeHaibTfbsK562Six5Pcr1xPkRep2	0.000797	4.00E-03
256	wgEncodeSydhTfbsK562Brg1IggmusPk	0.000766	2.00E-03
257	wgEncodeOpenChromFaireK562OhureaPk	0.000764	4.00E-03
258	wgEncodeHaibTfbsK562Mef2aV0416101PkRep1	0.000673	6.99E-03
259	wgEncodeBroadHistoneK562RestPk	0.000653	1.60E-02
260	wgEncodeSydhTfbsK562Bdp1StdPk	0.000643	4.00E-03
261	wgEncodeHaibMethylRrbsK562HaibSitesRep2	0.000618	9.99E-04
262	wgEncodeHaibMethylRrbsK562HudsonalphagrowprotSitesRep2	0.000618	9.99E-04
263	wgEncodeHaibTfbsK562SrfV0416101PkRep2	0.000568	3.00E-03
264	wgEncodeSydhTfbsK562MaffIggrabPk	0.000529	9.99E-03
265	wgEncodeSydhTfbsK562Gata1UcdPk	0.000524	3.00E-03
266	wgEncodeHaibTfbsK562Sin3ak20V0416101PkRep1	0.000471	3.00E-03
267	wgEncodeSydhTfbsK562CjunIfng30StdPk	0.000458	3.00E-03

268	wgEncodeSydhTfbsK562Sirt6StdPk	0.000414	1.30E-02
269	wgEncodeHaibTfbsK562Bclaf101388Pcr1xPkRep2	0.000377	9.99E-03
270	wgEncodeSydhTfbsK562Nfe2StdPk	0.000338	9.99E-04
271	wgEncodeSydhTfbsK562CjunIfng6hStdPk	0.000289	1.30E-02
272	wgEncodeSydhTfbsK562NelfeStdPk	0.000257	2.00E-02
273	wgEncodeSydhTfbsK562Ini1IggmusPk	0.000233	3.00E-02
274	wgEncodeSydhTfbsK562Tf3c110StdPk	0.000223	9.99E-04
275	wgEncodeHaibTfbsK562Taf7sc101167V0416101PkRep2	0.000212	8.99E-03
276	wgEncodeSydhTfbsK562Atf3StdPk	0.000173	5.00E-03
277	wgEncodeHaibTfbsK562Bcl3Pcr1xPkRep1	0.000125	4.00E-03
278	wgEncodeHaibTfbsK562Mef2aV0416101PkRep2	0.000114	2.40E-02
279	wgEncodeHaibTfbsK562Bclaf101388Pcr1xPkRep1	0.00009	2.10E-02
280	wgEncodeSydhTfbsK562Setdb1UcdPk	0.000072	3.00E-02
281	wgEncodeHaibTfbsK562Taf7sc101167V0416101PkRep1	0.000032	1.80E-02
282	wgEncodeSydhTfbsK562Pol2s2StdPk	0.000003	9.99E-04

The score for similarity between our peaks and those of ENCODE K562 tracks, and the p-values, were calculated according to Methods.

Supplementary Material

Ullmark et al.

Table S5B, WT1 +KTS

	Track	Similarity score	p-value
1	wgEncodeOpenChromSynthK562Pk	0.003739	9.99E-04
2	wgEncodeHaibMethyl450K562SitesRep1	0.003115	9.99E-04
3	wgEncodeSydhTfbsK562Znf263UcdPk	0.002099	9.99E-04
4	wgEncodeBroadHistoneK562H3k4me1StdPk	0.001946	2.50E-02
5	wgEncodeBroadHistoneK562Chd1a301218aStdPk	0.001739	7.99E-03
6	wgEncodeBroadHistoneK562CtcfStdPk	0.001564	9.99E-03
7	wgEncodeSydhHistoneK562bH3k4me1UcdPk	0.001531	9.99E-04
8	wgEncodeSydhHistoneK562H3k4me1UcdPk	0.001531	9.99E-04
9	wgEncodeUwHistoneK562H3k27me3StdPkRep1	0.001092	9.99E-04
10	wgEncodeUwHistoneK562H3k27me3StdPkRep2	0.001065	9.99E-04
11	wgEncodeSydhHistoneK562bH3k27me3bUcdPk	0.00094	8.99E-03
12	wgEncodeSydhHistoneK562H3k27me3bUcdPk	0.00094	8.99E-03
13	wgEncodeBroadHistoneK562Cbx3sc101004Pk	0.000936	9.99E-04
14	wgEncodeHaibTfbsK562Mef2aV0416101PkRep1	0.000692	9.99E-04
15	wgEncodeSydhTfbsK562Znf143IggrabPk	0.000608	2.00E-03
16	wgEncodeHaibTfbsK562Pu1Pcr1xPkRep1	0.000549	2.00E-03
17	wgEncodeSydhTfbsK562Atf3StdPk	0.000548	3.80E-02
18	wgEncodeUwHistoneK562H3k36me3StdPkRep1	0.000535	9.99E-04
19	wgEncodeSydhTfbsK562Gata2UcdPk	0.000502	2.00E-03
20	wgEncodeUwHistoneK562H3k36me3StdPkRep2	0.000472	9.99E-04
21	wgEncodeSydhTfbsK562Setdb1UcdPk	0.000459	5.00E-03
22	wgEncodeBroadHistoneK562NcorPk	0.000441	9.99E-04
23	wgEncodeSydhTfbsK562CmycStdPk	0.000402	2.10E-02
24	wgEncodeHaibTfbsK562Mef2aV0416101PkRep2	0.000398	3.30E-02
25	wgEncodeSydhTfbsK562Pol2IggmusPk	0.000373	5.99E-03
26	wgEncodeBroadHistoneK562Chd4mi2Pk	0.000369	9.99E-04
27	wgEncodeHaibTfbsK562Sp1Pcr1xPkRep1	0.000298	4.20E-02
28	wgEncodeHaibTfbsK562Hey1Pcr1xPkRep1	0.000265	1.80E-02
29	wgEncodeSydhTfbsK562CfosStdPk	0.000261	1.40E-02
30	wgEncodeBroadHistoneK562PcafPk	0.000251	9.99E-04
31	wgEncodeHaibMethylRrbsK562HaibSitesRep1	0.000216	9.99E-04
32	wgEncodeHaibMethylRrbsK562HudsonalphagrowprotSitesRep1	0.000216	9.99E-04
33	wgEncodeHaibMethylRrbsK562HaibSitesRep2	0.000212	9.99E-04
34	wgEncodeHaibMethylRrbsK562HudsonalphagrowprotSitesRep2	0.000212	9.99E-04
35	wgEncodeSydhTfbsK562CjunStdPk	0.000203	2.70E-02
36	wgEncodeHaibTfbsK562Sp1Pcr1xPkRep2	0.0002	4.00E-03
37	wgEncodeHaibTfbsK562Hdac2sc6296V0416102PkRep2	0.000176	1.90E-02
38	wgEncodeHaibTfbsK562Gata2sc267Pcr1xPkRep2	0.000173	3.60E-02
39	wgEncodeHaibTfbsK562Ctcflsc98982V0416101PkRep2	0.000169	2.00E-03
40	wgEncodeSydhHistoneK562bH3k9acbUcdPk	0.00016	1.20E-02
41	wgEncodeSydhHistoneK562H3k9acbUcdPk	0.00016	1.20E-02
42	wgEncodeBroadHistoneK562Suz12051317Pk	0.000155	9.99E-04
43	wgEncodeHaibTfbsK562Ctcflsc98982V0416101PkRep1	0.000094	3.20E-02
44	wgEncodeSydhTfbsK562Rad21StdPk	0.000086	4.60E-02
45	wgEncodeSydhTfbsK562E2f6UcdPk	0.000082	4.10E-02
46	wgEncodeSydhTfbsK562CjunIggrabPk	0.000057	4.00E-03
47	wgEncodeSydhTfbsK562Usf2IggrabPk	0.000047	3.30E-02
48	wgEncodeBroadHistoneK562Sirt6Pk	0.000045	9.99E-04
49	wgEncodeHaibTfbsK562Stat5asc74442V0422111PkRep1	0.000034	9.99E-03
50	wgEncodeHaibTfbsK562NrsfV0416102PkRep2	0.000023	4.00E-02
51	wgEncodeSydhTfbsK562Gtf2f1ab28179IggrabPk	0.000018	5.99E-03

52	wgEncodeHaibTfbsK562Cebpbsc150V0422111PkRep2	0.000016	3.80E-02
53	wgEncodeHaibTfbsK562Atf3V0416101PkRep2	0.000015	5.00E-02
54	wgEncodeSydhHistoneK562bH3k4me3bUcdPk	0.000009	4.30E-02
55	wgEncodeSydhHistoneK562H3k4me3bUcdPk	0.000009	4.30E-02
56	wgEncodeHaibTfbsK562Cbx3sc101004V0422111PkRep2	0.000007	4.10E-02
57	wgEncodeHaibTfbsK562Taf1V0416101PkRep1	0.000006	3.60E-02
58	wgEncodeHaibTfbsK562Cebpdsc636V0422111PkRep1	0.000004	6.99E-03
59	wgEncodeHaibTfbsK562Trim28sc81411V0422111PkRep1	0.000003	3.60E-02

The score for similarity between our peaks and those of ENCODE K562 tracks, and the p-values, were calculated according to Methods.

---

3. FIGURES

3.1 Supplementary Fig S1.

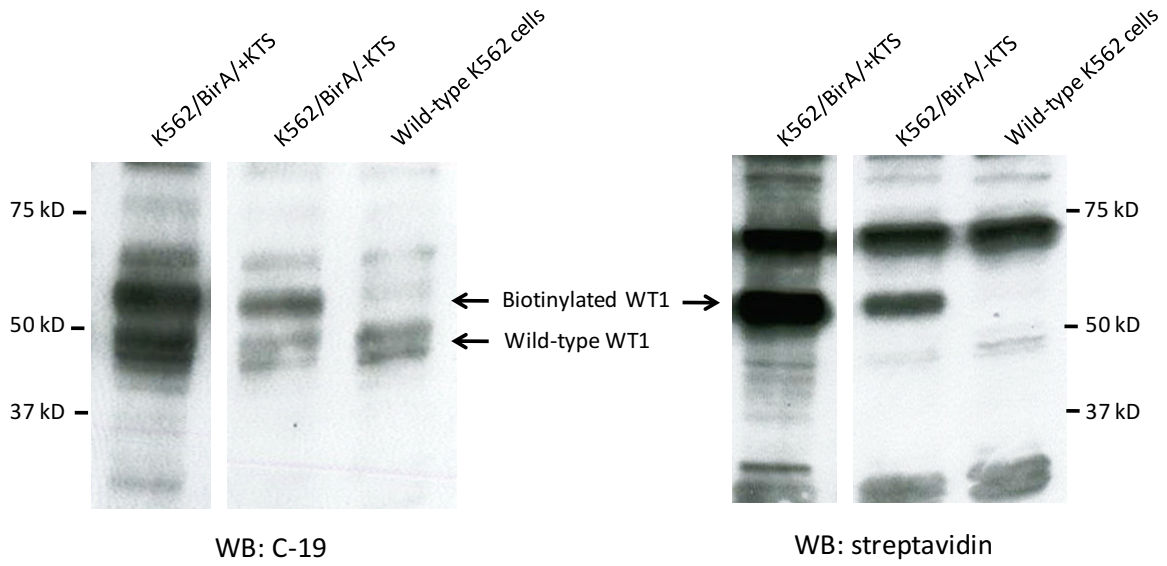

Supplementary Fig S1. Clones carrying biotinylated FLAGBIO-tagged WT1 -KTS were chosen for comparable expression of tagged and endogenous WT1. Cells were transfected through electroporation with pEF1α*BirA*V5-neo plasmid, and positive monoclones were selected for with G418 treatment. One such monoclone was then transfected through electroporation with pEF1αFlagbiotin-(*WT1* -KTS)-puro or pEF1αFlagbiotin-(*WT1* +KTS)-puro plasmid, and positive monoclones were selected for by adding puromycin to the treatment. Cells were harvested, lysed and subjected to Western blot analysis using WT1 antibody (Santa Cruz), and Streptavidin-HRP conjugate (Invitrogen), as described in Material and methods.

Supplementary Material

Ullmark et al.

3.2 Supplementary Fig S2.

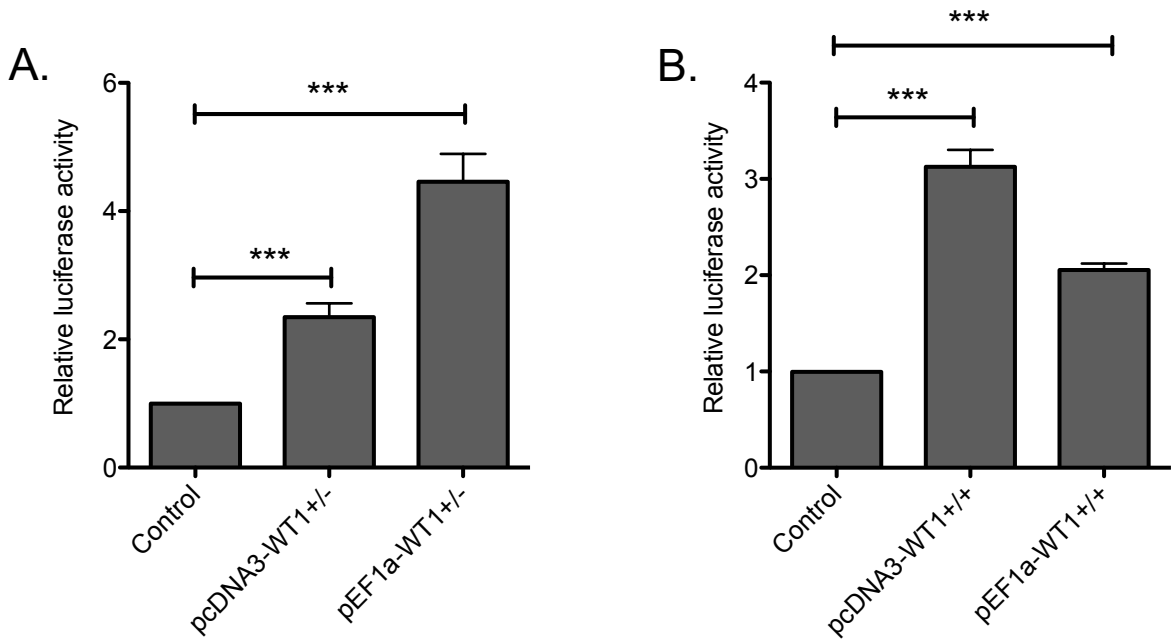

Supplementary Fig. S2. FLAGBIO-tagged WT1 -KTS is functional. 293T/17 cells were transfected with a luciferase reporter construct containing the minimal promoter for the Vitamin D receptor, together with pcDNA3 -WT1-KTS, pcDNA3-WT1 +KTS, pEF1a-FLAGBIO-WT1 -KTS, pEF1a-FLAGBIO-WT1 +KTS, or, or empty pcDNA3 as control, as indicated. Cells were lysed and subjected to luciferase analysis, reflecting the degree of activation of the VDR promoter (±S.E.M, n=4).

Supplementary Material

Ullmark et al.

3.3 Supplementary Fig S3.

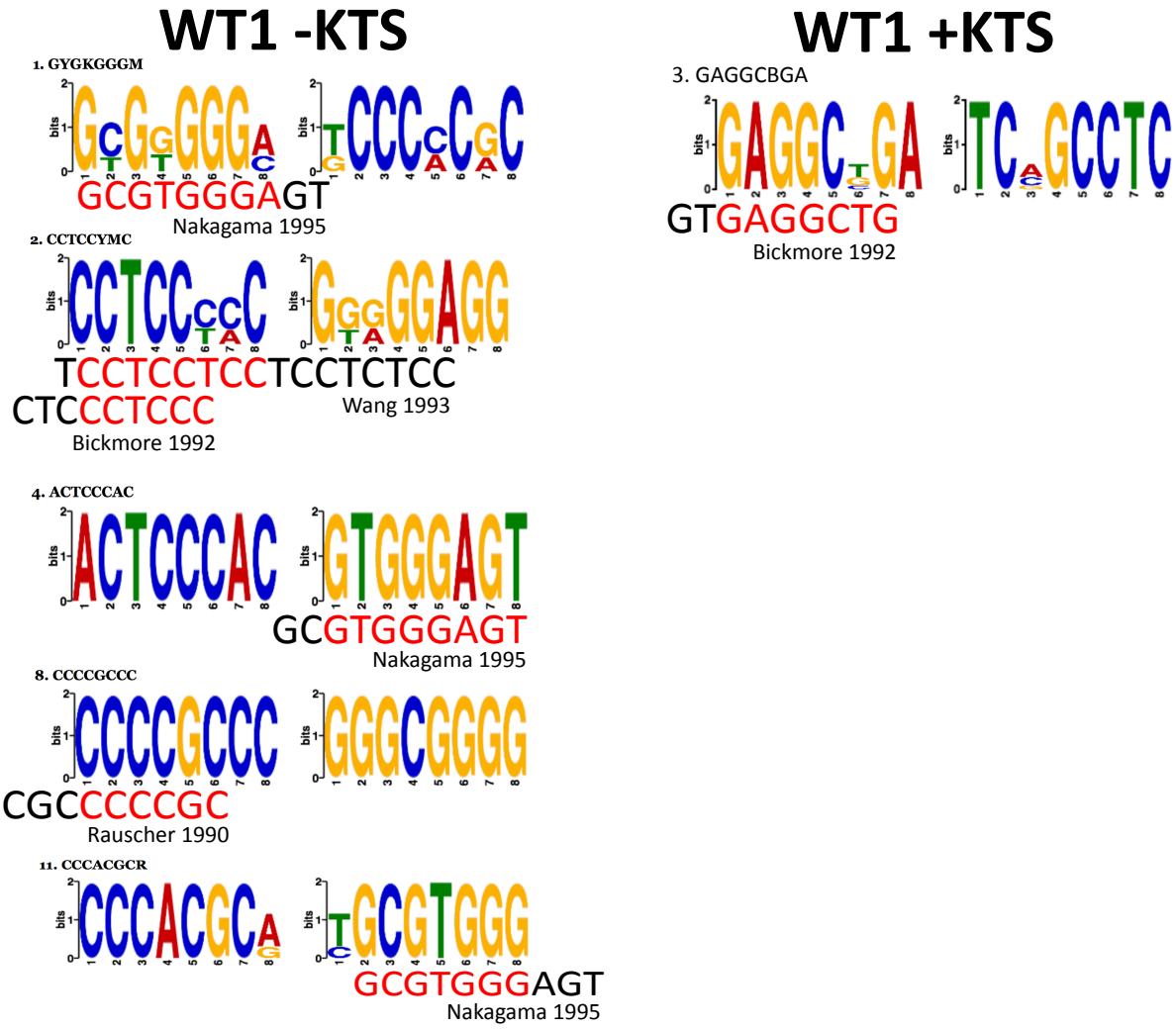

Supplementary Fig. S3. Motifs found in WT1 peaks compared with previously published WT1 motifs. Shown are both the positive and the complementary string, with the matching motif and reference article below.

References:

Bickmore WA, Oghene K, Little MH, Seawright A, van Heyningen V, Hastie ND. Modulation of DNA binding specificity by alternative splicing of the Wilms tumor wt1 gene transcript. Science. 1992;257:235-7.

Nakagama H, Heinrich G, Pelletier J, Housman DE. Sequence and structural requirements for high-affinity DNA binding by the WT1 gene product. Mol Cell Biol. 1995;15:1489-98.

Wang ZY, Qiu QQ, Enger KT, Deuel TF. A second transcriptionally active DNA-binding site for the Wilms tumor gene product, WT1. Proc Natl Acad Sci U S A. 1993;90:8896-900.

Rauscher FJ 3rd, Morris JF, Tournay OE, Cook DM, Curran T. Binding of the Wilms' tumor locus zinc finger protein to the EGR-1 consensus sequence. Science. 1990;250:1259-62.